FINAL REPORT

SBS APPLICATIONS STUDY

CONTRACT N00014-91-C-0246

January 1992

prepared for

OFFICE OF NAVAL RESEARCH
ARLINGTON, VA

prepared by

GTE GOVERNMENT SYSTEMS CORPORATION
MOUNTAIN VIEW, CA

TABLE OF CONTENTS

LIST OF ILLUSTRATIONS

LIST OF TABLES

Section 1
INTRODUCTION AND SUMMARY

This document is the Final Technical Report prepared by GTE Government Systems Corporation for the Office of Naval Research to document the work performed on Contract N00014-91-C-0246. The thrust of the research was to investigate the potential feasibility of remote sensing applications of stimulated Brillouin scattering (SBS) in water.

GTE Government Systems Corporation has previously conducted exploratory research into the use of Brillouin scattering for remote underwater sensing with DARPA sponsorship via Office of Naval Research Contracts N00014-87-C-0739 and N00014-89-C-0049. An important result of this prior work was the experimental demonstration that a very large percentage (≈50%) of the incident laser energy could be converted into a phase-conjugate stimulated Brillouin scattering (SBS) Stokes-shifted return beam which was so well collimated that it could be easily detected at a very high signal-to-noise ratio (SNR) by a receiver co-located with the laser transmitter.

The potential applications for ocean remote sensing using SBS that were considered in this study are shown in Table 1-1.

Table 1-1
Underwater Applications for SBS

• DETECTION AND MEASUREMENT OF ACOUSTIC WAVES
• DETECTION AND MEASUREMENT OF TURBULENCE
• DETECTION AND MEASUREMENT OF INTERNAL WAVES
• MEASUREMENT OF SOUND VELOCITY PROFILES

The underwater measurements can be made from the SBS return beam in either of two fundamentally different ways, i.e., by means of (1) the frequency shift or (2) the phase shift. Section 2 discusses the use of the SBS technique in the various applications areas and estimates are made for the performance that can be achieved. It is shown that precision SBS measurements in regimes of interest are feasible in the areas of turbulence, internal waves and sound velocity profiles but that the measurement of coherent acoustic waves by means of SBS remains a high risk endeavor.

The precision of an SBS remote sensing measurement depends upon the linewidth of the SBS beam. Research was conducted to investigate the method of broadband seeding as a means to narrow the SBS linewidth and thereby to improve the precision of the measurement. This work is described in Section 3. The investigation included both experimental measurements and the development of a descriptive model of the seeding process for analysis of the experimental results.

Recommendations for further research in the area of SBS measurement applications are given in Section 4.

Section 2

SURVEY OF POTENTIAL SBS APPLICATIONS

Each of the various SBS application areas shown in Table 1-1 makes use of a uniquely different physical signature. These signatures and how they may be detected by the SBS process are described in the following.

2.1 DETECTION AND MEASUREMENT OF ACOUSTIC WAVES

An acoustic wave, as it passes by a fixed underwater location consists of a succession of compressions and expansions of the water. Also the sound wave causes a succession of back and forth particle motions. These physical effects, the density changes and the particle velocity changes are the effects that will influence the SBS signal. The SBS frequency shift will be a function of both the water density and the longitudinal particle velocity. The phase shift of a beam reflected from the SBS mirror will be a function of the density integral that the reflected beam has traversed. Two possible geometries to measure the phase shift using the SBS mirror are shown in Figure 2-1. The magnitude of these effects is calculated in the following.

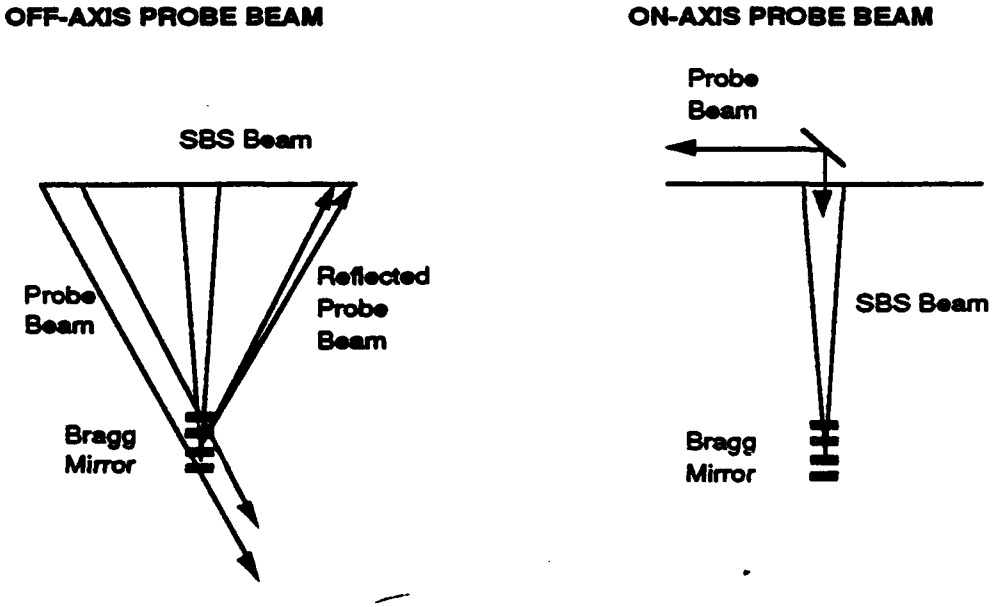

Figure 2-1 SBS Phase Shift Measurement Geometries

2.1.1 Phase Shift vs. Sound Wave Pressure

The compressibility of liquid water is 5×10^{-5} atm^{-1} i.e. for liquid water $\Delta V/V = 5 \times 10^{-5} \Delta P$. This expression relates the fractional change in volume $\Delta V/V$ to a change in pressure ΔP. In terms of the standard units that are used in underwater acoustics ΔP is usually expressed in units of dB re: 1 μPa. Table 2-1 shows the RMS fractional volume change $\Delta V/V$ as a function of pressure expressed both in terms of dynes/cm^2 and in dB re: 1μPa. This relationship between sound pressure and water compression is essentially independent of the sound frequency.

Table 2-1

Water Compression vs. Sound Pressure

SOUND WAVE RMS PRESSURE		COMPRESSION RATIO
(dB re: 1 Pa)	(dynes/cm2)	ΔV/V
120	10	5E-10
100	1	5E-11
80	0.1	5E-12
60	0.01	5E-13
40	0.001	5E-14
20	0.0001	5E-15

This modulation of the water density, or equivalently the modulation of the index of refraction of the water, by the sound wave will have an effect on the optical path difference and thus the phase of the received light. A geometry such as shown in Figure 2-1 is assumed. The optical path difference (OPD) and the phase difference $\Delta\Phi$ are given by the expressions:

$$OPD = (n_o + \Delta n)\, L - n_o\, L = \Delta n\, L$$

and $\Delta\Phi = OPD\ (2\pi/\lambda)$

where

n_o = refractive index without a sound wave present
Δn = rms refractive index modulation due to sound wave
L = physical underwater path of light
λ = wavelength of light

The index of refraction (n) can be written in terms of the density of water (ρ)

$$n = 1 + 0.33\ (\rho/\rho_o)$$

Since $\Delta V/V = \Delta\rho/\rho_o$ an expression for Δn can be obtained by substitution.

$$\Delta n = 0.33\ \Delta V/V = 1.7 \times 10^{-11}\ \Delta P$$

If the roundtrip pathlength, L, in the water is 10 meters, and a wavelength λ of 532 nm is used then the change in the number of wavelengths due to the sound pressure is

$$(\Delta n\, L/\lambda) = 1.7 \times 10^{-11}\ \Delta P\ (10/532 \times 10^{-9}) = 3.2 \times 10^{-4}$$

wavelengths for 100 dB sound pressure. Expressing in terms of RMS phase

$$\Delta\Phi = 2\pi \times 3.2 \times 10^{-4} = 0.002 \text{ radians}$$

or $\Delta\Phi = 360 \times 3.2 \times 10^{-4} = 0.12$ degrees.

The signal-to-noise ratio (SNR) that is required to determine phase with a given RMS precision is the following:

$$\Delta\Phi = 1 / (\sqrt{SNR}) \text{ , radians}$$

The SNR is related to heterodyne received power by the expression

$$SNR = q\, P / h\upsilon\, B = N_{pe}$$

where q = quantum efficiency

P = received optical power

$h\upsilon$ = energy per photon

B = bandwidth

N_{pe} = number of photoelectrons collected

By substitution therefore, the expression

$$\Delta\Phi = 1 / (\sqrt{N_{pe}})$$

can be written which relates the number of photoelectrons to the required phase precision. Table 2-2 shows, for a pathlength of 10 m and a wavelength of 532 nm the relationship between sound pressure and the expected $\Delta\Phi$ and the minimum required SNR and the corresponding minimum number of photoelectrons N_{pe} that must be collected, in the shot noise limit.

Table 2-2

SNR Required to Measure Phase Shift

RMS SOUND PRESSURE (dB re: 1μPa)	RMS PHASE SHIFT (radians)	SNR	PHOTOELECTRONS Npe
120	2.00E-02	2.50E+03	2.50E+03
100	2.00E-03	2.50E+05	2.50E+05
80	2.00E-04	2.50E+07	2.50E+07
60	2.00E-05	2.50E+09	2.50E+09
40	2.00E-06	2.50E+11	2.50E+11
20	2.00E-07	2.50E+13	2.50E+13
Path Length = 10 m		Wavelength = 532 nm	

2.1.2 SBS Frequency Shift and Sound Waves

There are two effects associated with sound waves that would affect the SBS frequency which are: (1) the effect of pressure on sound speed and (2) the Doppler effect of the longitudinal particle velocity.

2.1.2.1 Pressure Effects on SBS Frequency Shift

A modulation of the water density by the sound wave will modulate the bulk sound speed of the water and thus the Brillouin shift. The rate of change of Brillouin frequency with sound speed is ≈ 5 MHz per m/s, and the rate of change of sound speed with water pressure is ≈ 1.6 E-7 m/s per dyne/m^2. Thus the rate of change of Brillouin frequency with water pressure is ≈ 0.8 Hz per dyne/m^2. The Brillouin frequency shift as a function of sound pressure level is given in Table 2-3.

Table 2-3

SBS Frequency Shift by Sound Pressure

SOUND WAVE RMS PRESSURE		SBS FREQUENCY SHIFT
(dB re: 1 Pa)	(dynes/cm2)	Δf (Hertz)
120	10	8
100	1	0.8
80	0.1	0.08
60	0.01	0.008
40	0.001	0.0008
20	0.0001	0.00008

2.1.2.2 Particle Velocity Effects on SBS Frequency Shift

The particle velocity in water due to the presence of a sound wave can be related to the sound wave RMS pressure by the acoustic impedance of liquid water which is 1.5 E+5 gm/cm^2-s. Therefore u = 7 E-6 P where P is the sound wave RMS pressure in dynes per cm^2 and u is the particle velocity in cm/s. Again using the fact that the rate of change of Brillouin frequency shift is 5 MHz per m/s the SBS frequency shift can be easily calculated and the results are shown in Table 2-4.

Table 2-4

SBS Frequency Shift by Sound Particle Velocity

SOUND WAVE RMS PRESSURE		SBS FREQUENCY SHIFT
(dB re: 1 Pa)	(dynes/cm2)	Δf (Hertz)
120	10	3.5
100	1	0.35
80	0.1	0.035
60	0.01	0.0035
40	0.001	0.00035
20	0.0001	0.000035

2.2 DETECTION AND MEASUREMENT OF TURBULENCE

The longitudinal component of turbulent velocity fluctuations will, through the Doppler effect, appear as fluctuations in the observed SBS frequency shift. The rate of change of Brillouin frequency with Doppler velocity is ≈ 5 MHz per m/s. The SBS frequency fluctuation as a function of turbulent water velocity fluctuations is thus easily calculated and is given in Table 2-5.

Table 2-5

SBS Frequency Fluctuation vs Velocity Fluctuation

VELOCITY	SBS FREQUENCY SHIFT
(m/s)	(MHz)
1	5
0.1	0.5
0.01	0.05
0.001	0.005

2.3 DETECTION AND MEASUREMENT OF INTERNAL WAVES

Internal waves are characterized by very slow movement of subsurface water that has a vertical density gradient typically as a result of a vertical temperature

gradient. Such waves are especially common in or near the depth of the thermocline.

The detection of internal waves is accomplished by measurement of the subsurface density (or temperature) field in 3 dimensions. The very slow motion of the water precludes practical use of Doppler effects. The 3-dimensional density structure can be detected with SBS either by means of the phase shift technique of by the effect of the density on the bulk sound speed of the water, and thus on the observed SBS frequency shift.

2.3.1 Phase Shift Determination of Internal Waves

The density structure of the internal waves will assume to be related to temperature variations. (An analogous development could be stated for salinity effects.) The rate of change of density of liquid water with respect to temperature is $\approx 2 \times 10^{-4}$, i.e. $\Delta V/V = 2 \times 10^{-4} \Delta T$ where ΔT is in °C.

In Section 2.1.1, the rate of change of index of refraction with respect to density was derived as $\Delta n = 0.33\ \Delta V/V$. By substitution, index changes can be related to temperature changes as $\Delta n = 6.8 \times 10^{-5} \Delta T$. Further following the development in Section 2.3.1, and assuming that the roundtrip pathlength, L in the water is 10 meters, and the wavelength is 532 nm, then the change in the number of wavelengths due to a temperature change ΔT is

$$(\Delta n\ L/\lambda) = 6.8 \times 10^{-5} \Delta T\ (10/532 \times 10^{-9})$$

For a 1 °C temperature change $(\Delta n\ L/\lambda) = 1.2 \times 10^{3}$ wavelengths, which when expressed in terms of phase is

$$\Delta\Phi = 2\pi \times 1.2 \times 10^{3} = 7.5 \times 10^{3} \text{ radians}$$

For practical phase measurements with the highest accuracy it is desirable that the phase difference being measured is of order π radians. One way in which this can be accomplished is to use a tunable laser and measure the phase difference as the laser wavelength is varied. For a variation of $\Delta\lambda$ the phase difference is smaller than the original phase

shift by a factor of $\Delta\lambda/\lambda$. This is shown for wavelengths λ_1 and λ_2 that are separated by $\Delta\lambda$ by the following:

$$\Delta(\Delta\Phi_2 - \Delta\Phi_1) = \Delta n L \{(1/\lambda_1) - (1/\lambda_2)\} \approx (\Delta n L/\lambda)(\Delta\lambda/\lambda)$$

For the above example with $\Delta T = 1°C$ and a pathlength of 10 m the phase shift of 7500 radians can be measured as a difference of π radians if the value of $\Delta\lambda/\lambda$ is set at 0.0004 which means that at a nominal wavelength of 532 nm the laser would have to be tuned by 0.2 nm. These relationships are shown in Figure 2-2 which is

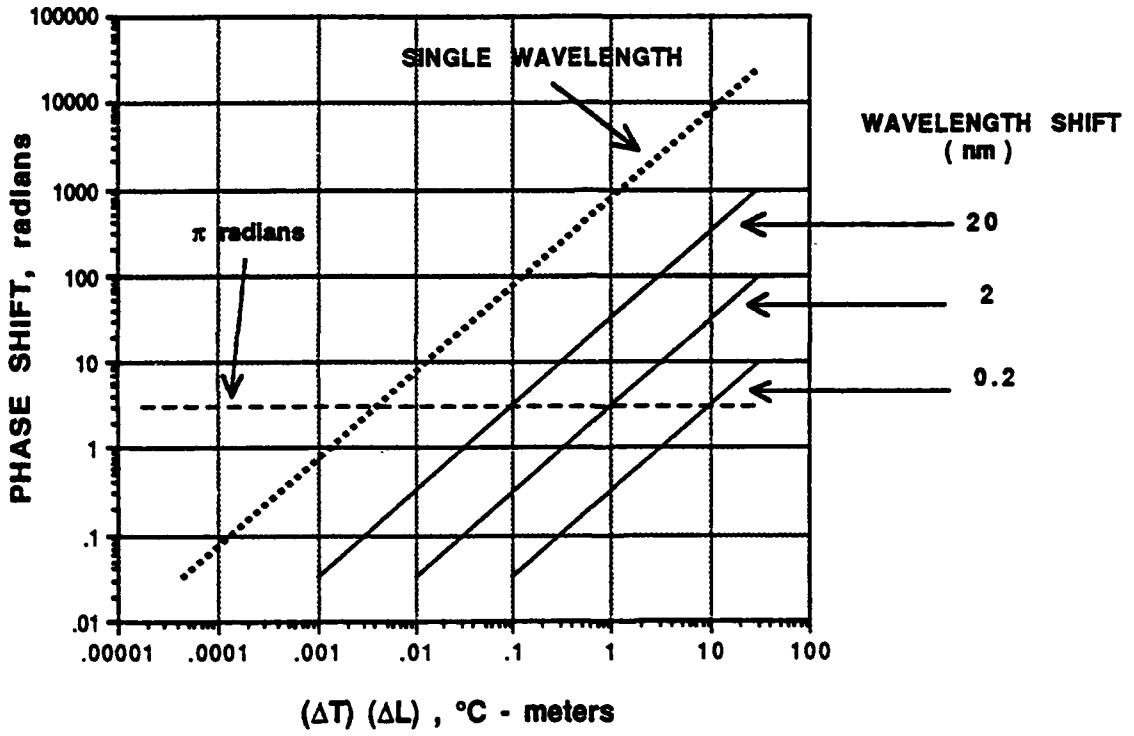

Figure 2-2 Phase Shift vs (ΔT) (ΔL)

a map that shows the phase shift in radians as a function of the $\Delta T \Delta L$ temperature pathlength product with wavelength tuning as a parameter. By appropriately adjusting the wavelength shift, the original value of phase shift for a single wavelength can be

transformed into a phase shift difference of $\approx \pi$ radians.

The accuracy of the measurement is given by the expression for RMS phase error that was developed in Section 2.1.1 which is

$$\Delta\Phi = 1 / \sqrt{(SNR)} = 1 / \sqrt{(N_{pe})}$$

For example with a SNR = 10^6, the RMS accuracy of the phase shift measurement would be a milliradian. which for a 10 m pathlength and 1 °C temperature would correspond to a 1 millidegree temperature accuracy.

2.3.2 SBS Frequency Shifts.

The bulk sound speed of the water can be used as a "tracer" for the water density and thus enable detection of internal waves. The Brillouin frequency shift is a direct measure of sound speed, which in most circumstances is a strong function of temperature. The rate of change of Brillouin frequency with water temperature is ≈15 MHz / °C. Table 2-6 shows the relationship between temperature change and Brillouin frequency shift.

Table 2-6

Water Temperature Change vs SBS Frequency Shift

TEMPERATURE	SBS FREQUENCY SHIFT
(°C)	(MHz)
1	15
0.1	1.5
0.01	0.15
0.001	0.015

2.4 MEASUREMENT OF SOUND VELOCITY PROFILE

Optimization of acoustic systems requires a 3-dimensional data base of sound velocity. The measurement can be made in either of two ways: (1) by means of SBS frequency shifts, with an accuracy as shown in Table 2-6; or (2) by means of optical phase shift measurements, with an accuracy as given in Figure 2-2.

Section 3
BROADBAND SEEDING OF SBS IN WATER

This Section describes the investigation that was carried out on broadband seeding of stimulated Brillouin scattering (SBS) in water. The objective of this work was to determine by experimental measurement the parameter space, including seed energy and water particulate loading, in which seeding by broadband backscattering could be used to narrow the SBS frequency. The investigation included experimental measurements and the development of a descriptive model of the seeding process for analysis of the experimental results. Tests showed that even in distilled water broadband seeding could be used to narrow the SBS frequency distribution.

3.1 DESCRIPTION OF EXPERIMENTAL SETUP - OPTICS

Laboratory experiments were conducted to demonstrate broadband seeding of phase conjugate stimulated Brillouin scattering (SBS) with the seeding being carried out from the sensor side of the probe volume. Previous seeding experiments from the reverse side had shown that broadband seeding could significantly narrow the distribution of the SBS mean frequency value from pulse to pulse.

The GTE-provided laboratory setup for the experiments is shown in Figure 3-1. The laser source is a Spectra-Physics Model 6300-DCR-3 Nd:YAG with injection locking which when doubled produces a transform limited pulse in the green at 530 nm which has a FWHM of 7 ns and a frequency bandwidth of 140 MHz. The laser typically operates at 10 Hz over a range of pulse energy from 1 mJ to 100mJ.

As indicated in Figure 3-1, the output of the laser is directed by mirror M1 to beamsplitter BS1 which splits off a laser reference beam. The laser reference beam is directed by mirrors M2 and M3 to fiber optic launcher FL1. This beam is used as the reference frequency against which the Brillouin frequency shift of the SBS beam that is produced by water cell #1 and collected by fiber launcher FL2 is measured.

The remainder of the original laser beam that passes through beam splitter BS1 is further split into two portions by beam splitter BS2. One portion, used as the

pump beam for the SBS production in water cell #1, is directed by mirrors M4, M5 and M6 and focused into water cell #1. The SBS beam that is produced is captured by beam splitter BS3 and directed by mirror M8 to fiber optic launcher FL2. The optical

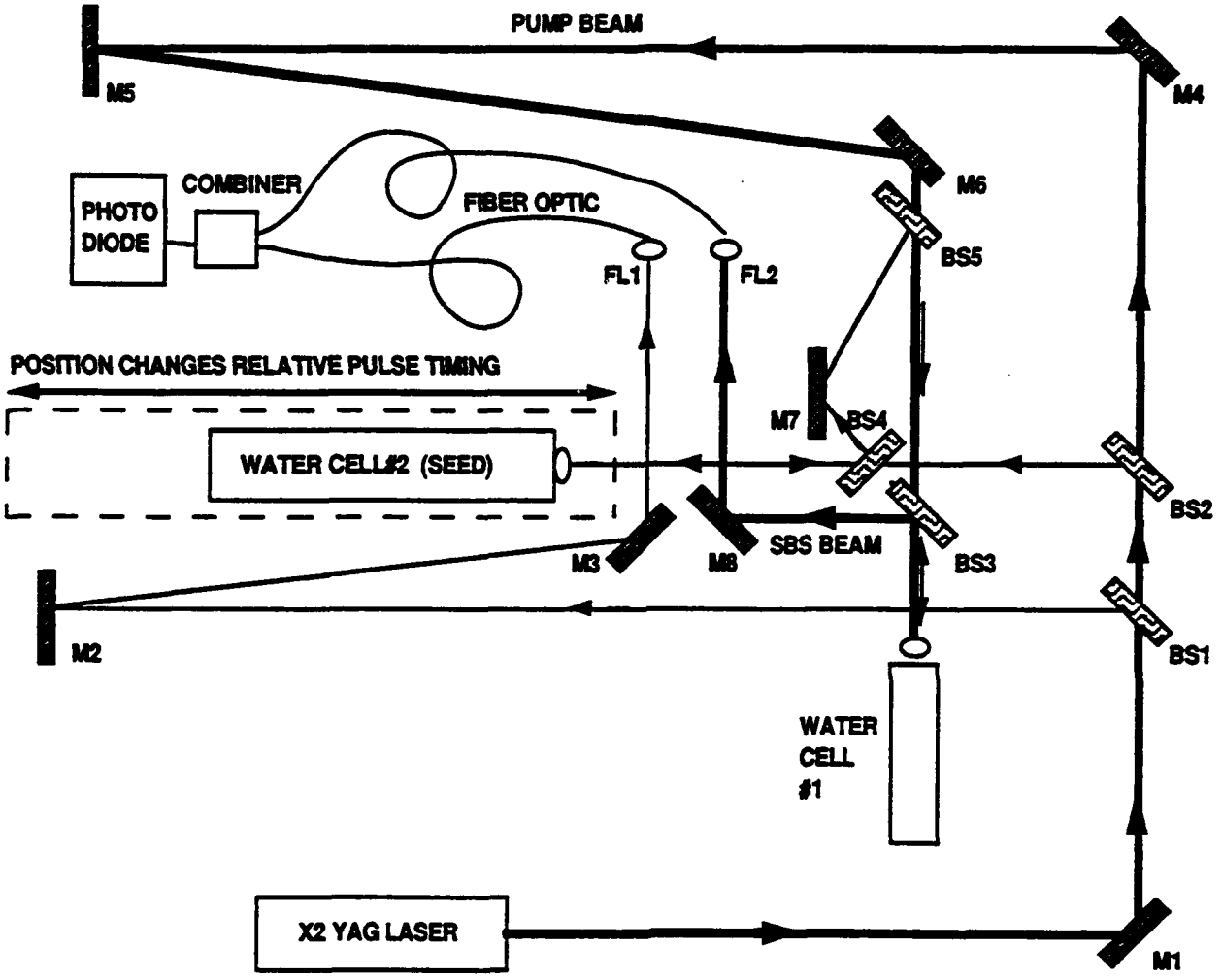

Figure 3-1 Laboratory Setup for Seeding Experiments

pulses from F1 and F2 are combined in a fiber coupler and then detected by a photo diode. The Brillouin heterodyne beat frequency f(B) that is produced is then detected by standard discriminator electronic circuitry.

The other beam from beam splitter BS2 is directed to water cell #2 in which the broadband seed pulse is produced. The laser beam is focused very deeply in water cell #2, producing a very narrow SBS pulse of 0.5 ns or less in duration, which

is sufficiently broad band for proper seeding. The seed SBS pulse is directed to water cell #2 and aligned coaxial with the pump beam by beam splitters BS4 and BS5 and mirror M7. The timing of the seed pulse with respect to the pump pulse is critical for the proper functioning of the broadband seeding process. Adjustments in the timing were easily made by longitudinal translation of the water cell #2 and its focusing lens. Since the output seed pulse is the phase conjugate of the incoming beam no adjustment in angle of the seed beam was necessary even when the angular placement of water cell #2 was changed during the translational adjustments.

A shutter in the beam line between BS4 and BS5 enabled the seed pulse to be alternately present or not present so that its effect on the frequency width of the SBS pulse frequency distribution could be evaluated.

3.2 DESCRIPTION OF EXPERIMENTAL SETUP - DATA ACQUISITION

To observe and measure the Brillouin frequency [f(B) ≈ 7.7 GHZ at 20°C] which is contained in the heterodyne signal from the photodiode, a down converter circuit was employed. This circuit is shown in Figure 3-2. The output of the

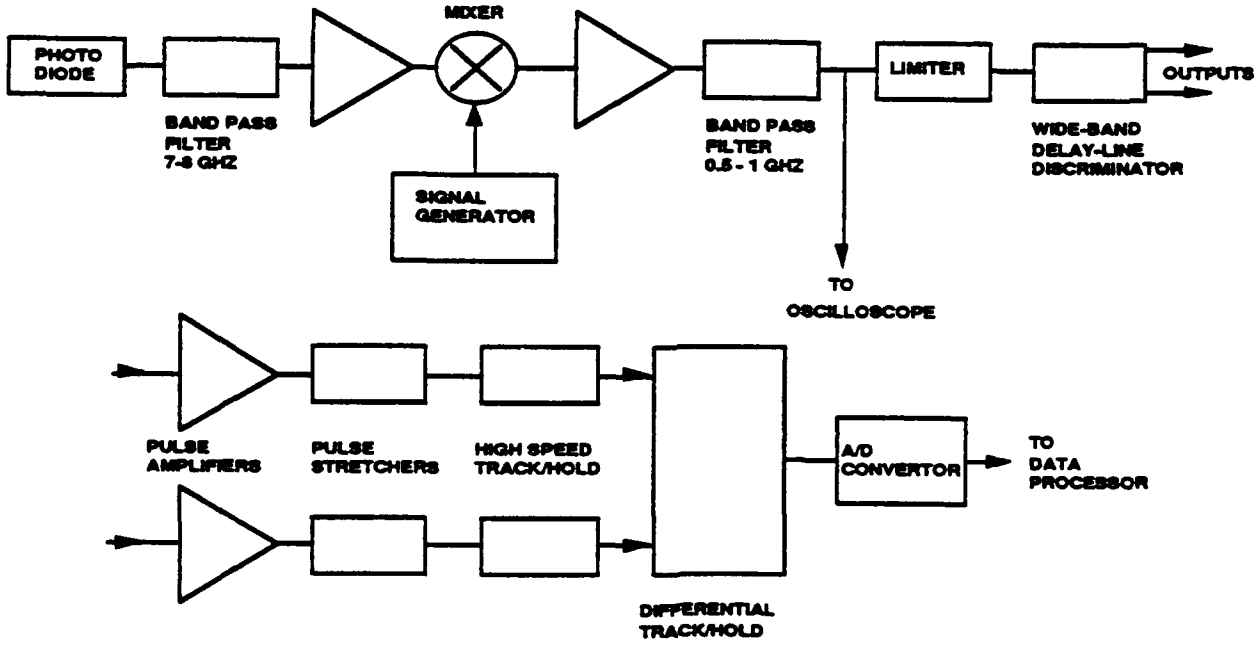

Figure 3-2 Experimental Setup for SBS Frequency Measurement

photodiode is suitably filtered and amplified before being mixed in a doubly balanced mixer. The resulting signal is placed in the 500 to 1000 MHz range by tuning the frequency of the signal generator. At this point the heterodyne signal may be observed directly on an oscilloscope. A Tektronix 7104 fitted with a 7A29 plug-in amplifier provided a realtime 1GHz bandwidth for observation of the heterodyne waveforms.

In addition to direct observation the signal was converted to an analog voltage for recording and processing. The conversion was accomplished by using a wide-band delay-line discriminator the differential output of which is proportional to the mean frequency during the pulse duration. After the two analog pulses from the discriminator are stretched and amplified, two high speed track-and-hold circuits are used to capture the peak level on each pulse. A differential track-and-hold circuit operating at a slower speed holds the differential analog for the entire interpulse period and is refreshed by the firing of the next laser pulse. The differential analog signal is converted to digital form in an A/D convertor for subsequent recording and processing by a HP 98458 desktop computer.

For each test, the mean frequency of several thousand SBS pulses was measured and recorded. Half of the SBS pulses in each test were produced with seeding and half without seeding. The HP processor calculated the standard deviation of the seeded and the unseeded sets of data for each test. In addition histograms were produced which graphically displayed the distribution of the mean SBS frequency for each test.

3.3 EXPERIMENTAL TEST RESULTS

The testing utilized spectroscopic grade, distilled water in Test Cell #1 for the purpose of establishing the sensitivity of the seeding process to the particulate loading of the water. Prior testing with the SBS broad-band seeding technique had utilized tap water in which significant particulate concentrations may have been present.

The broad pump and the narrow seed pulse shapes are both shown in the oscilloscope trace photograph in Figure 3-3. The time base is 2 ns per large division. The seed pulse half width is seen to be approximately 0.5 ns and may be limited by

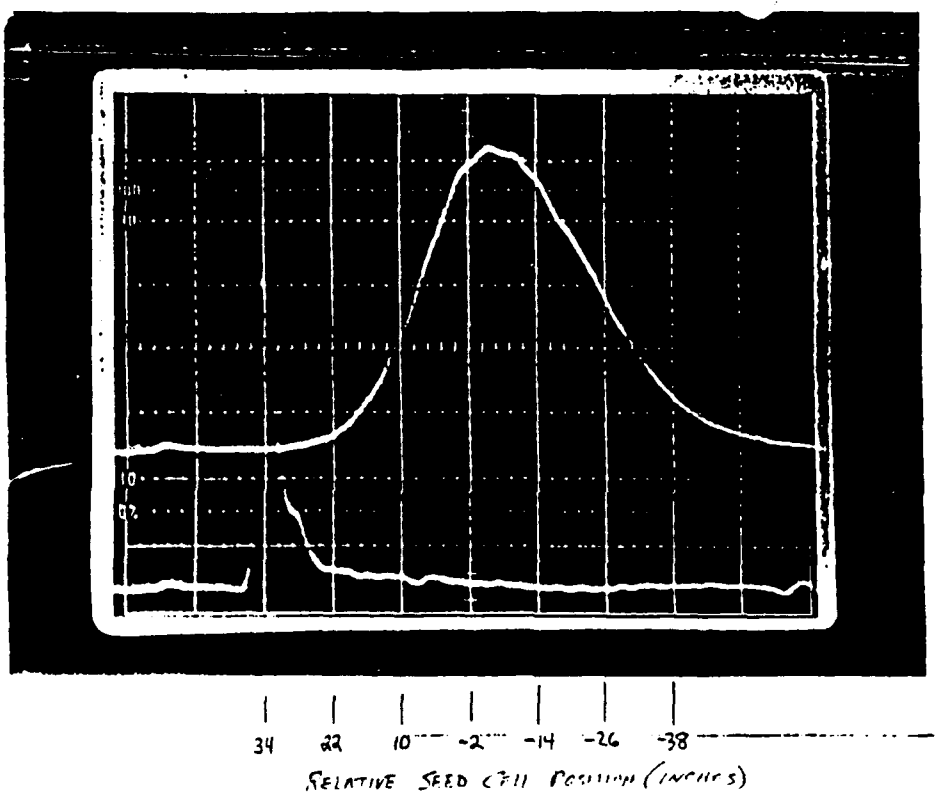

Figure 3-3 Oscillograph of Pump and Seed Pulse Shapes

the 1 GHz bandwidth of the scope. The pump pulse half width is approximately 5 ns.

The raw test data that was obtained is presented in Table 3-1. The entries in Table 3-1 are: (1) the run number; (2) the relative position of the seed cell, which determines the relative timing between the seed and the pump pulses, (a change of 6 inches in position corresponds to a change of 1 ns in relative timing because of the two way path in the arrangement of the experimental setup); (3) the ND attenuation in the seed beam; (4) the standard deviation of the SBS mean frequency for the seeded process; and (5) the standard deviation of the SBS mean frequency for the unseeded process.

For each of the 46 runs 1000 pulses were seeded and 1000 were unseeded. The data was obtained in alternating sequences of 100 seeded pulses followed by 100 unseeded pulses. Data sets with variable seed attenuation were obtained for each of four positions of the seed test cell, i.e., at the 12, 18, 24 and 30 inch locations. The relative pulse timing that these locations represent can be seen by the lower scale

Table 3-1

Raw Test Data Using Distilled Water

Run Number	Seed Cell Position (inches)	Seed Attn. (ND)	Std. Dev. Seeded	Std. Dev. Unseeded
1	7.5	0	0.0444	0.0748
2	12	0	0.0370	0.0692
3	12	0.3	0.0358	0.0608
4	12	0.6	0.0344	0.0551
5	12	0.9	0.0398	0.0553
6	12	1.3	0.0396	0.0499
7	12	2	0.0427	0.0448
8	- 6	0	0.1139	0.0658
9	12	0	0.0423	0.0624
10	12	0	0.0390	0.0759
11	18	0	0.0386	0.0752
12	18	0	0.0375	0.0733
13	24	0	0.0423	0.0766
14	30	0	0.0984	0.0753
15	34	0	0.1056	0.0790
16	27	0	0.0510	0.0780
17	-1.5	0	0.1645	0.0778
18	6	0	0.0482	0.0783
19	18	0.3	0.0402	0.0769
20	18	0.6	0.0394	0.0749
21	18	0.9	0.0388	0.0747
22	18	1.3	0.0420	0.0769
23	18	1.6	0.0425	0.0779
24	18	2	0.0401	0.0753
25	18	2.3	0.0439	0.0766
26	18	2.6	0.0421	0.0758
27	18	3	0.0516	0.0795
28	18	3.3	0.0541	0.0788
29	18	3.6	0.0784	0.0786
30	30	0.6	0.0622	0.0819
31	30	1.3	0.0459	0.0783
32	30	3	0.0734	0.0795
33	30	2.6	0.0720	0.0786
34	24	0.6	0.0385	0.0738
35	24	1.3	0.0349	0.0724
36	24	2.3	0.0480	0.0715
37	24	3	0.0583	0.0723
38	24	0	0.0404	0.0683
39	24	1.3	0.0341	0.0703
40	24	2.3	0.0490	0.0706
41	24	0	0.0406	0.0635
42	24	0.6	0.0368	0.0639
43	12	0	0.0344	0.0584
44	12	1	0.0411	0.0584
45	12	2	0.0462	0.0615
46	12	3	0.0477	0.0523

on Figure 3-3, with 30-inches being the earliest and 12-inches being the latest placement of the seed pulse relative to the pump pulse.

The ratio of the standard deviation of the seeded SBS process to the unseeded SBS process as a function of the ND attenuation in the seed beam with the seed cell position as a parameter is shown in Figure 3-4. This data shows that there is a preferred timing position for the seed pulse relative to the pump pulse and that this

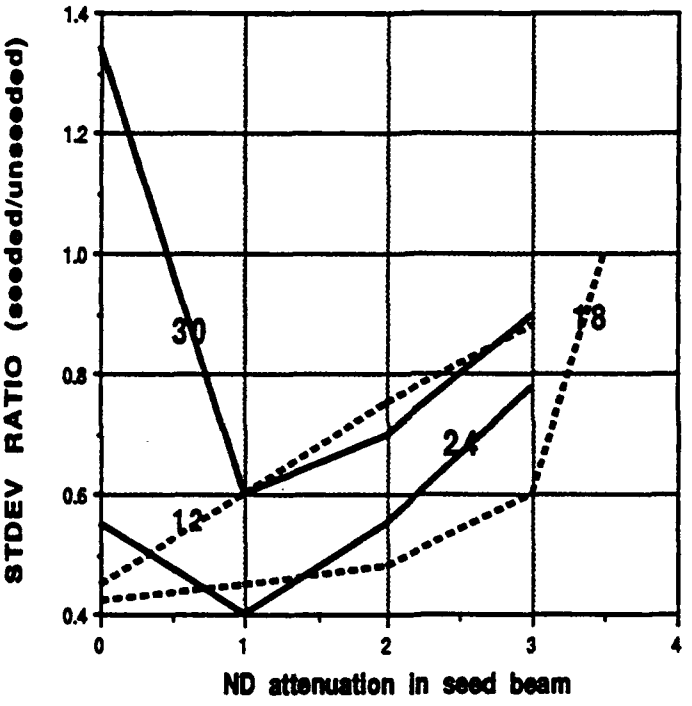

Figure 3-4 Reduction in Standard Deviation by Seeding

preferred position is a weak function of the seed energy. Under optimum conditions the standard deviations were reduced to 40% of the unseeded value. The data points for each of the four seed cell positions is shown separately in Figures 3-5 thru 3-8.

It is interesting to note that for seed timing before or after the optimum range the standard deviation when seeded was seen to increase to values greater than that

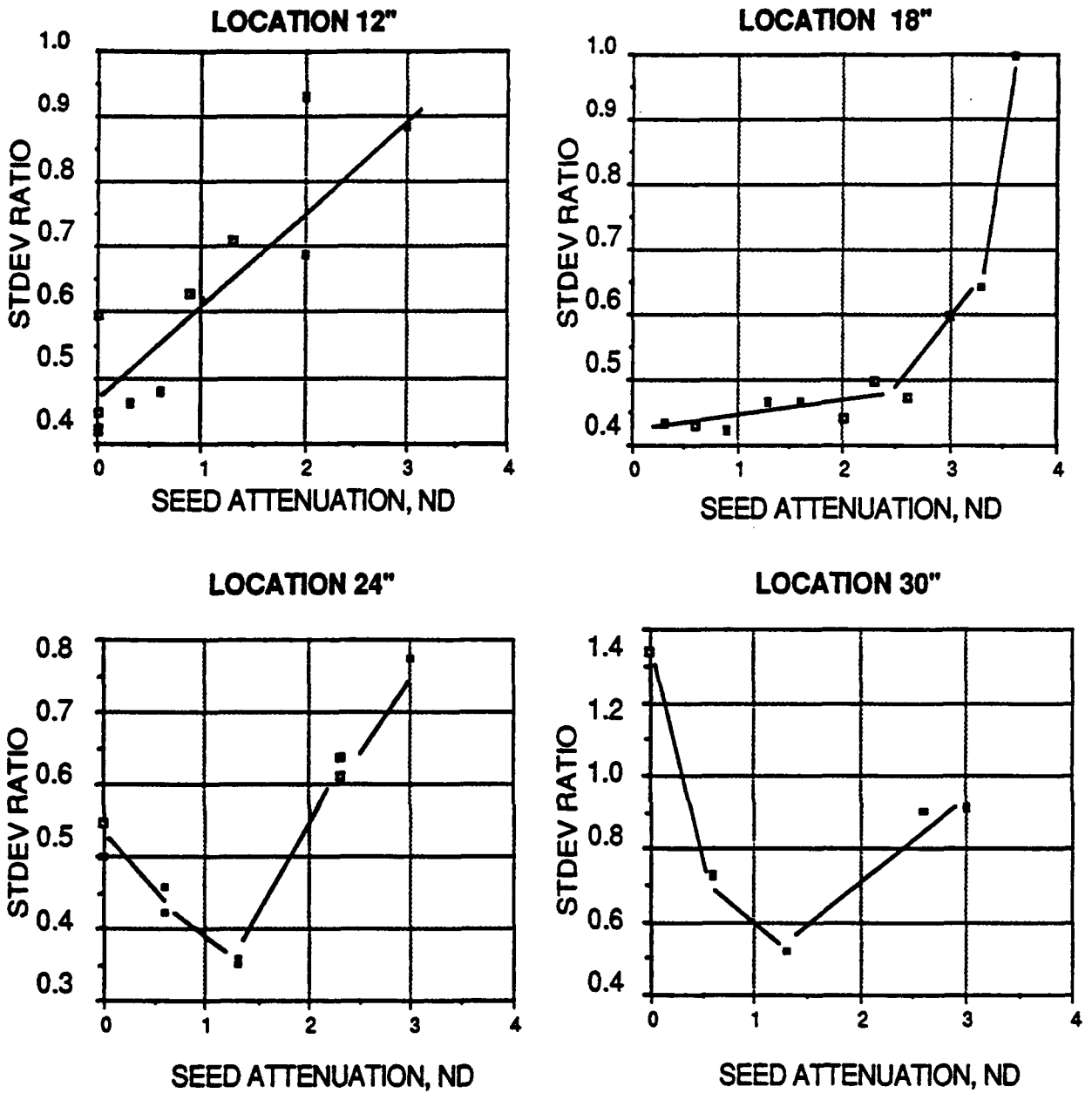

Figure 3-5 Reduction in Standard Deviation for Four Cell Positions

observed when unseeded.

Examples of the histograms obtained are shown in Figures 3-6 and 3-7 for the data obtained in runs #35 and #8 respectively. Figure 3-9 (run #35) shows the results of an optimum condition for seed pulse insertion in which the seeded histogram shows a significant narrowing of the SBS frequency distribution relative to the unseeded histogram. Figure 3-10 (run #8) shows a condition in which the seed pulse insertion

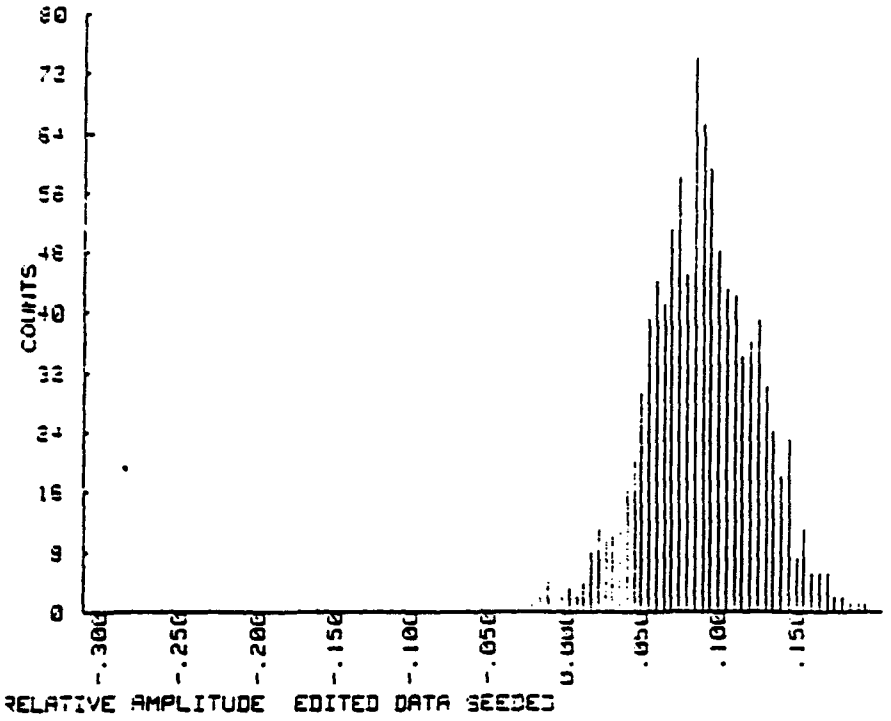

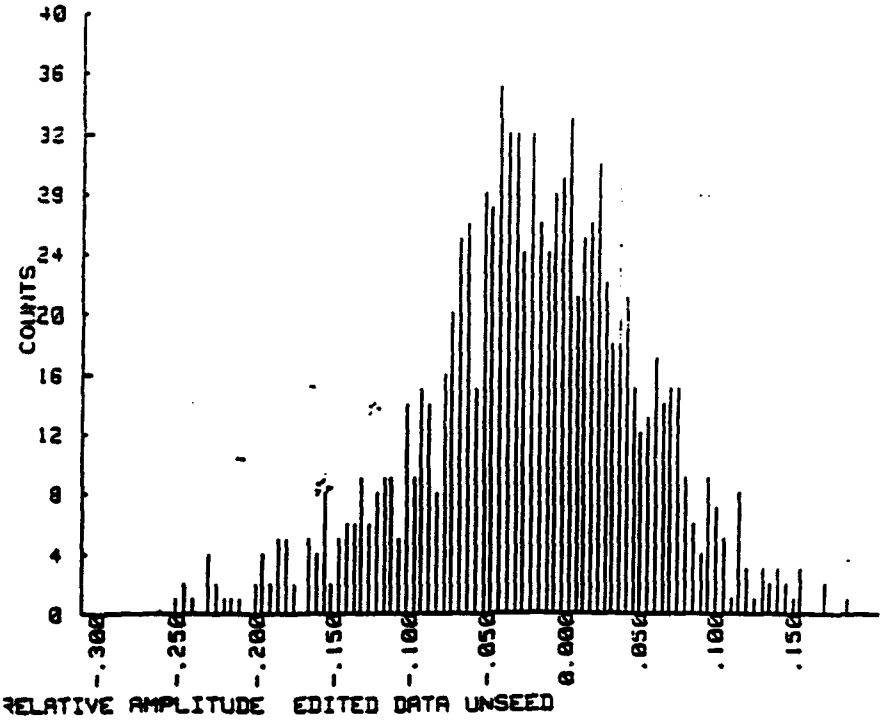

Figure 3-6 Histogram of Seeded SBS - Frequency Narrowed

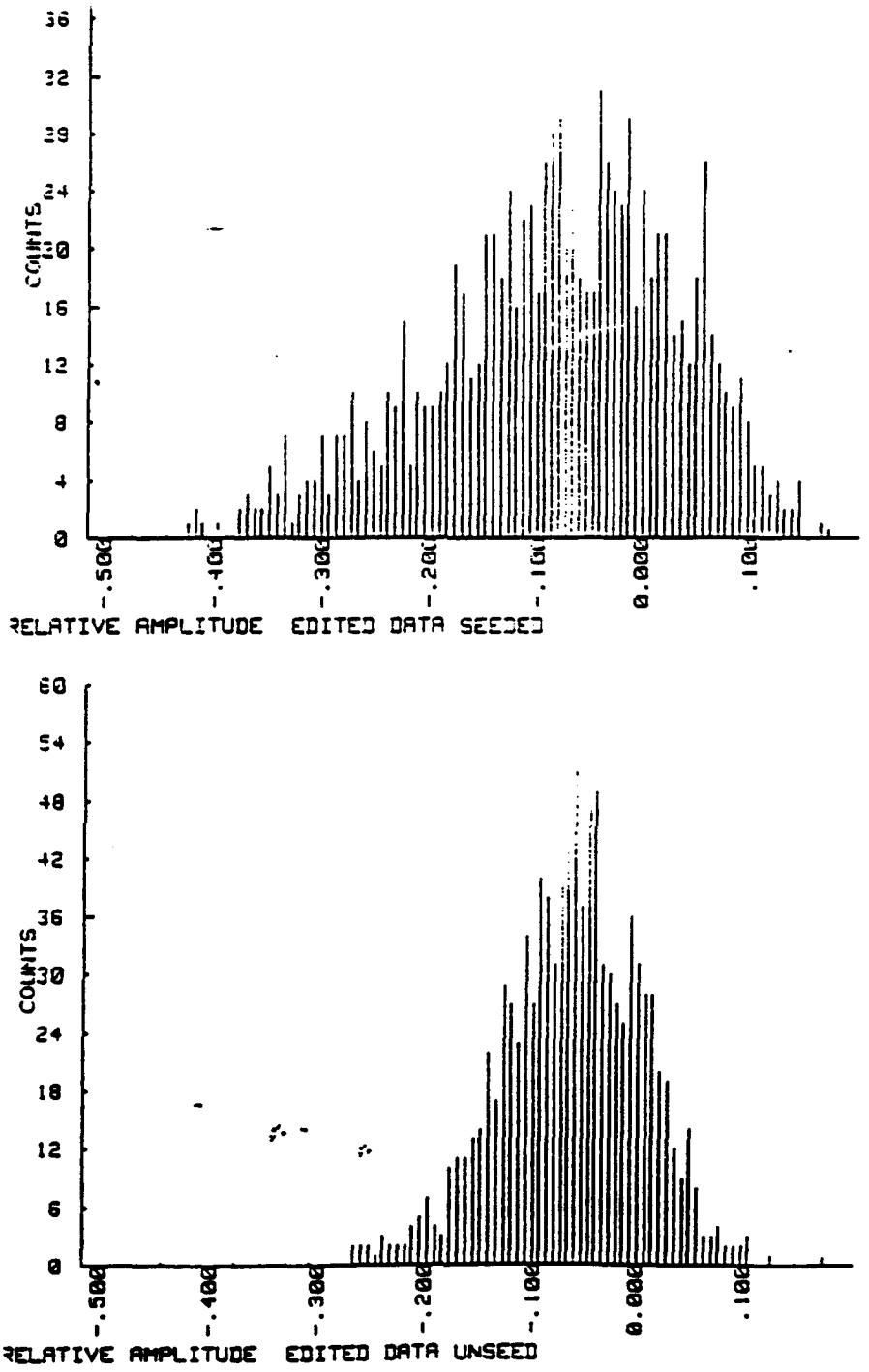

Figure 3-7 Histogram of Seeded SBS - Frequency Broadened

occurs later than optimum, and a broadening of the seeded histogram relative to the unseeded histogram is observed. This broadening is interpreted as a reflection of the seed pulse from the mature SBS region with subsequent detection of the broadband SBS seed frequencies in addition to the pump pulse derived SBS frequencies.

3.4 ANALYSIS OF TEST RESULTS WITH RESPECT TO SEED ENERGY

The backscattered seed intensity can be calculated from the following general expression:

$$I_S(bs) = I_S(o)\ \beta\ \Delta l\ \Delta\Omega$$

where $I_S(bs)$ = backscattered seed intensity

$I_S(o)$ = incident seed intensity

β = backscatter coefficient, $m^{-1}sr^{-1}$

Δl = effective path length for seed backscatter, m

$\Delta\Omega$ = effective solid angle for seed backscatter, sr

Two basic assumptions are now invoked:

Assumption #1 - A diffraction limited optical system is used to focus both the seed and pump beams.

Assumption #2 - The seed beam becomes effective when ≈ 1 seed photon is present.

With the assumption that a diffraction limited optical system is being used, and the effective path length for seed backscatter is the length of the focal waist, then the product $\Delta l\ \Delta\Omega$ can be written as

$$\Delta l\ \Delta\Omega = 4.8\ \lambda$$

since $\Delta l = 4.8\ \lambda\ (f\#)^2$ and $\Delta\Omega = (f\#)^{-2}$ and therefore the expression for the backscattered seed intensity becomes

$$I_S(bs) = I_S(o)\ 4.8\ \beta\ \lambda$$

which it should be noted is independent of f#.

The magnitude of the backscatter coefficient ß is dependent on the level of the particulate loading in the water. For zero particulate concentration (a condition difficult to produce even in the laboratory) the backscatter consists of a triplet, two symmetrically shifted Brillouin lines and a center unshifted line. The ratio of the intensity of the unshifted center line to the Brillouin line intensity in pure water is calculable from basic physical principles and is known as the Landau-Placzek (LP) ratio. The LP ratio is usually written as $I_c/2I_b$ where I_c is the center intensity and I_b is the Brillouin intensity. At 20 °C the ratio $I_c/2I_b = 8 \times 10^{-3}$.

The minimum effective seed energy is calculated by setting the expression for the backscatter seed intensity equal to one photon. Therefore

$$1 = (1/h\upsilon)\, I_S(bs) = (1/h\upsilon)\, I_S(o)\, ß\, \Delta l\, \Delta\Omega$$

and

$$I_S(o) = h\upsilon / 4.8\, ß\, \lambda$$

where

$$ß = (I_c/I_b)\, ß\,(B) = 2 \times 8 \times 10^{-3} \times 1 \times 10^{-4} = 1.6 \times 10^{-6}\ m^{-1}\ sr^{-1}$$

$$\lambda = 0.532 \times 10^{-6}\ m^{-1}$$

$$h\upsilon = 3.8 \times 10^{-19}\ J.$$

Therefore

$$I_S(o) = (3.8 \times 10^{-19}) / (4.8 \times 1.6 \times 10^{-6} \times 0.532 \times 10^{-6}) = 9.3 \times 10^{-6}\ J$$

is the theoretical energy needed to produce 1 photon of effective backscatter seed intensity.

The experimentally observed minimum seed energy that was effective occurred with an attenuation of ND=3 of a 0.6 mJ pulse which corresponds to a pulse energy of 6×10^{-7} J.

Figure 3-8 displays this information as a log-log plot of seed pulse energy in µJ vs. the backscatter coefficient normalized to the value for distilled water. The line on this plot with a slope of -1 labeled "calculated for 1 photon" represents the above calculated value of $I_S(o)$ scaled inversely proportional to the backscatter coefficient ß.

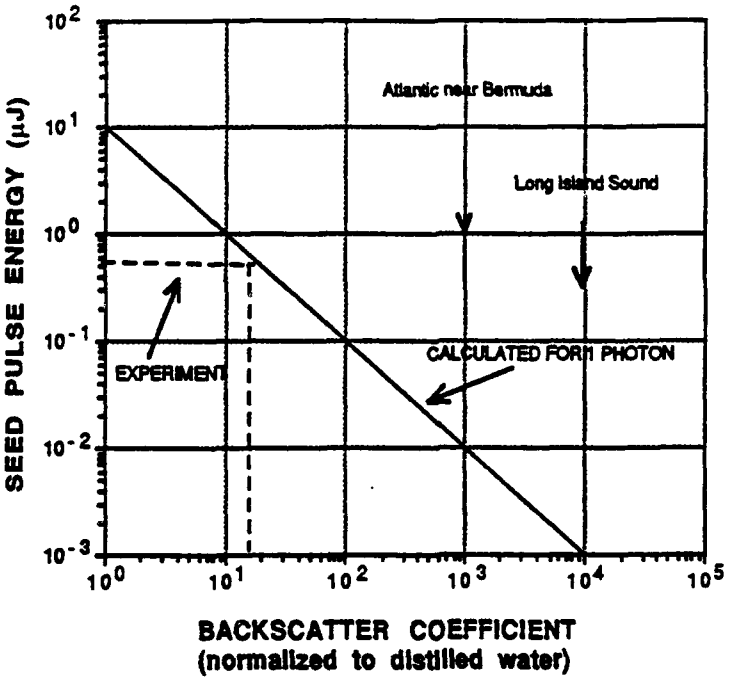

Figure 3-8 Seed Energy Required vs. Backscatter Coefficient

The horizontal dashed line labeled "experiment" shows the experimentally determined value of the seed energy which is needed for effective seeding. The vertical dashed line, determined by the intersection of the horizontal "experiment" line with the calculated line for 1 photon, indicates the actual value of the backscatter coefficient for the distilled water. The higher value for backscatter coefficient than the LP ratio for water means that the distilled water was contaminated with dust, a not improbable likelihood since the water cells were not filled under clean room conditions.

Also shown in Figure 3-8 are the values of backscatter coefficient likely to be encountered in open ocean (near Bermuda) and in coastal waters (Long Island Sound). For these values of backscatter coefficient the data indicates that there would be more than adequate backscattering for effective seeding.

Section 4
RECOMMENDATIONS

The feasibility of the use of the SBS process in certain subsurface remote sensing applications has been shown feasible. It is recommended that further development activities be pursued. These results and recommendations are summarized in Table 4-1. The descriptive categories in Table 4-1 are defined as follows: (1) Compelling - can solve an existing problem in a straightforward manner

Table 4-1
Recommendations for SBS Remote Sensing

APPLICATION	SBS MEASUREMENT TECHNIQUE	
	FREQUENCY	PHASE
SOUND WAVES		
Pressure	N/A	HIGH RISK
Velocity	HIGH RISK	N/A
TURBULENCE		
Velocity	INTERESTING	N/A
INTERNAL WAVES		
Density	INTERESTING	COMPELLING
SOUND VELOCITY PROFILES		
Temperature/Salinity	COMPELLING	COMPELLING

with high sensitivity. The Navy should move out smartly to make use of the technique; (2) Interesting - the technique has potential and with further development the utility may be proven; (3) High Risk - the technique appears to lack the needed sensitivity. A breakthrough is needed to show feasibility.

It is recommended that conceptual system designs be developed for the internal wave and sound velocity profile applications that are deemed to be compelling. This design effort should be followed by key proof-of principle experiments.